J. Electroanal. Chem., 199 (1986) 323–340
Elsevier Sequoia S.A., Lausanne – Printed in The Netherlands

CLAY MODIFIED ELECTRODES

PART VI. ALUMINUM AND SILICON PILLARED CLAY-MODIFIED ELECTRODES

WALTER E. RUDZINSKI * and ALLEN J. BARD

Department of Chemistry, The University of Texas, Austin, TX 78712 (U.S.A.)

(Received 3rd September 1985)

ABSTRACT

Metal (Ru, Os, Fe) bipyridyl complexes and $Ru(NH_3)_6^{3+}$ were incorporated into several montmorillonite clays and their aluminum and silicon-pillared analogues. Film concentrations and apparent diffusion coefficients were measured and compared by using spectrophotometry, cyclic voltammetry and chronocoulometry. The catalytic role of isomorphously substituted iron was evaluated and implicated by its effects on $Ru(bpy)_3^{3+}$ voltammetric behavior. A model is proposed for charge transport within the novel silicon-pillared clay.

INTRODUCTION

Na-montmorillonite and Na-hectorite possess a layered structure in which two-dimensional oxyanions are separated by a layer of hydrated cations [1,2] (Fig. 1). The oxyanion layer consists of two silicate inverted tetrahedral sheets sharing their apical oxygen with an octahedral sheet. The 2:1 relation between the tetrahedral and octahedral sheets within a layer allows the smectite clays to be classified as 2:1 phyllosilicates. In the electroneutral mineral pyrophyllite, a dioctahedral 2:1 phyllosilicate, two out of three of the octahedral sites are occupied by aluminum, whereas in talc, all three octahedral sites are occupied by magnesium [2]. Substituting 15% of the Al(III) by Mg(II), or 8% of the Mg(II) by Li(I), results in the commonly observable structures of montmorillonite and hectorite, respectively [1]. Since there is a positive charge deficiency in the oxyanion layer of smectites ranging from 0.4 to 1.2 e per Si_8O_{20} [2], layers of hydrated cations are intercalated between the silicate sheets. In natural clays, the intercalated cations are usually alkaline earth ions (Ca^{2+}), but sometimes alkali metal ions (Na^+). These cations are exchangeable, and because the layer lattice structure is expandable, ions and large molecules can

* Present address: Department of Chemistry, Southwest Texas State University, San Marcos, TX 78666, U.S.A.

0022-0728/86/$03.50 © 1986 Elsevier Sequoia S.A.

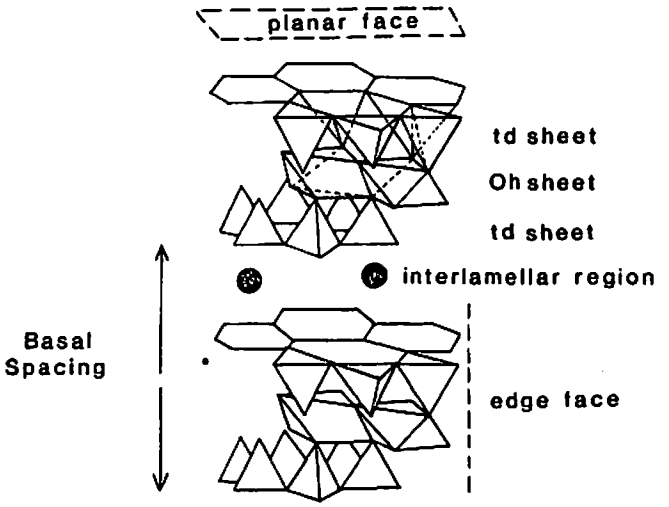

Fig. 1. Representation of the structure of a 2:1 phyllosilicate.

penetrate between the sheets, resulting in increased basal spacings. Large organic molecules in particular can penetrate and orient themselves along the plane of the silicate sheet [3].

Swelling phyllosilicate minerals (smectite clays) have been employed recently as thin film supports for electroactive cations [4,5]. Both montmorillonite and hectorite clays have been used to prepare colloidal suspensions which are then cast on a conductive electrode surface. A variety of probe ions, including metal bipyridyl complexes or bipyridinium derivatives, have been used to investigate the electrochemical activity of clay-modified electrodes [4,5]. In this paper, we evaluate the influence of the type of clay and the nature of the intercalated cation on the overall rate of charge transport through the clay film. Measurement of the apparent diffusion coefficient, D_0, and film concentration, c_0, for $Ru(NH_3)_6^{3+}$, $Fe(bpy)_3^{2+}$, $Ru(bpy)_3^{2+}$, and $Os(bpy)_3^{2+}$ (where bpy = 2 2'bypyridine) in Texas montmorillonite (STx-1), and hectorite (SHCa-1), was used to provide insight into the mechanism of charge transport within the clay.

A second goal of this research was to prepare robust clay films that would neither collapse in aprotic solvents (or at high temperature) nor expand and delaminate in dilute aqueous solution. By fixing the spacing of the interlamellar region, smectites can maintain an interlayer spacing of between ca. 0.3 nm and 1.0 nm, and because of their rigidity, discriminate among substrates on the basis of size or shape, much like faujasitic zeolites. Recently the development of pillared-clay modified electrodes has been reported [4e], where polynuclear oxycations of aluminum, zirconium and iron were incorporated, followed by heat treatment which then induces the formation of "pillars" that crosslink the 2:1 phyllosilicate layers. Such robust pillared-clay modified electrodes feature ca. 1.7 nm basal spacing, good rigidity, and the ability to sustain charge transport in nonaqueous solution.

We extend the work on pillared-clay modified electrodes by reporting diffusion coefficients and film concentrations for the aluminum-pillared clay and a novel silicon-pillared clay. These data were compared with those obtained on unpillared clay-modified electrodes to elucidate the effect of pillaring on the overall charge transfer rate. In addition, the synthetic route adopted for pillaring silicon may provide a general route for the intercalation of a variety of organosilicon compounds within smectite clays.

Finally, smectite clays have the ability to function as catalysts because of: (1) the high proton activity of water molecules within the interlamellar region [6], (2) the ability of smectites to intercalate catalytically active metal complexes [2], and (3) the presence of sites within a smectite that can act as oxidants (as in the conversion of benzidine hydrochloride or tetrathiafulvalene to its respective cation [3a–c], or as reductants (e.g., converting tetracyanoethylene (TCNE) to the radical anion [3a,d]). Structural iron may be involved in such charge transfer processes [3c,e]. This oxidizing or reducing property of the clay support can enhance the peak currents observed in cyclic voltammetry (CV), and lead to additional complexity in the interpretation of voltammetric data. To assess the role of immobilized iron in the CV response, four clays with different iron contents were evaluated for their effect on the electrochemistry of $Ru(bpy)_3^{2+}$ and $Ru(NH_3)_6^{3+}$.

EXPERIMENTAL

Materials

Wyoming montmorillonite (SWy-1) was purified using a method described in a previous paper [4c]. Texas montmorillonite (STx-1) and (SHCa-1) hectorite were purified using a modification of the procedure described previously [4c]. 10–20 g of clay were dispersed in 1 l of 1 *M* NaCl for at least 48 h to exchange the Ca^{2+} ions with Na^+. The clay suspensions were then centrifuged for 5 min (IEC table top centrifuge) and the supernatant discarded. The precipitate was then re-suspended in water and re-centrifuged twice. Removal of excess Cl^- was continued by dialysis (tubing from Spectrapor, Spectrum Medical Industries, Inc.) until a negative test for Cl^- ions with 0.1 *M* $AgNO_3$ was obtained. The clay was then centrifuged at high speed (5,000 rpm) for at least 15 min. The dark sediment was discarded, and the colloidal solution decanted and stored. The colloidal solution was then either freeze-dried or used without further treatment. Alternatively, STx-1 was purified according to ref. 4d. A nontronite suspension was obtained from Dr. H. Hartman (Department of Earth Sciences, Massachusetts Institute of Technology, Cambridge, MA) and used without further purification. Tris(2,2′-bipyridyl)ruthenium(II) chloride hexahydrate [$Ru(bpy)_3Cl_2\ 6H_2O$] was obtained from Strem Chemicals (Newbury, MA). $Ru(NH_3)_6Cl_3$ was obtained from Aldrich (Milwaukee, WI). $Os(bpy)_3(ClO_4)_2$ and $Fe(bpy)_3(ClO_4)_2$ were synthesized and purified according to published procedures [7a,b]. LiCl, NaCl, KCl, tetramethylammonium chloride (TMACl) and tetraethylammonium chloride (TEACl), Na_2SO_4 and $K_4Fe(CN)_6$

were used as received. Distilled water for all experiments was from a Milipore water purification system. Hydroxy-aluminum solution $[Al(OH)_2Cl]_x$, for the preparation of aluminum-pillared clay, was prepared by slowly adding with vigorous stirring 0.05 *M* NaOH to 0.1 *M* $AlCl_3$ to give an OH^- to Al(III) ratio of 2 : 1 [8]. The solution was then allowed to sit for 2 d to allow formation of the oligomer [9]. Tetraethoxysilane $[Si(OC_2H_5)_4]$ was obtained from Petrarch (Bristol, PA).

Methods

All thin clay films were prepared by spin-coating 10 drops of a (50 : 50) ethanol-water colloidal suspension on 1 cm^2 Nesatron (In_2O_3) conducting glass (PPG Industries, Pittsburgh, PA). The conducting glass was spun at 8000 rpm using a photo-resist spinner (Headway Research Inc., Garland, TX) and was heated with a heat gun for 15 s before applying the clay solution. The film thickness was ca. 50 nm before impregnation of electroactive cation, and ca. 100 nm after use. Both values were determined by using profilometry.

Several approaches were used to prepare aluminum-pillared clays: (1) STx-1 or SHCa-1 spin-coated on Nesatron, was soaked for up to 18 h in 0.02 *M* $[Al(OH)_2Cl]_x$; the sample was rinsed with water and then heated at 300–400°C for 3 h, followed by soaking in supporting electrolyte for 45 min (saturation approach). (2) 5 ml of 0.02 m*M* $[Al(OH)_2Cl]_x$ were added to 5 ml of STx-1 (10 g/l); the mixture was allowed to react overnight, and the sample was then heated, allowing water to evaporate until a gelatinous precipitate formed. This was then coated on Nesatron to produce a film thickness of ca. 1 μm. (3) A 1 μm thick clay film was soaked for 18 h in 0.02 *M* $[Al(OH)_2Cl]_x$, after which the sample was rinsed, then heated at 350°C for 2.5 h.

Two different approaches were used for the preparation of silicon-pillared clay modified electrodes: (1) STx-1, SWy-1, or SHCa-1 was spin-coated on Nesatron, soaked for a minimum of 3 h in neat tetraethoxysilane $[Si(OCH_2CH_3)_4]$ under a dry atmosphere, then heated at 300–400°C for at least 3 h (saturation approach). (2) A STx-clay was spin-coated on Nesatron, soaked for 15 h in a solution consisting of (1 : 1 : 10)v/v dry ethanol + tetraethoxysilane + CH_2Cl_2, then heated at 350°C for 3 h. Electroactive cations were incorporated into the thin film by soaking for at least 10 min (and up to 30 min) in 1–5 m*M* solution of the metal complex.

Equipment

X-ray diffraction data were obtained with a General Electric (model xrd-5) X-ray power diffractometer using the copper kα line as the source, graphite as the monochromator, and an Ortec (model 401A) ratemeter as the counting device. The copper anode was operated at 35 kV and 20 mA while the counter was set at either 300 or 1000 counts s^{-1} with a time constant of 1 s. Films for these measurements were usually ca. 10 μm thick. Profilometry was performed using a Sloan-Dektak profilometer.

Absorption spectra were obtained on a Hewlett-Packard model 8450A dual beam spectrophotometer. Solution spectra were obtained in 1 cm quartz cuvets, whereas film spectra were obtained directly on the coated Nesatron electrodes.

Cyclic voltammetry experiments were performed using a Princeton Applied Research (PAR) model 175 universal programmer and a model 173 potentiostat. Voltammograms were recorded on a Houston Instruments 2000 X–Y recorder. Chronocoulometry was performed using a Bioanalytical Systems (Lafayette, IN) BAS-100 electrochemical analyzer. All electrochemical experiments were performed in an undivided three-electrode cell with a 30 ml volume. Working electrodes were Nesatron conductive glass (0.5–1.0 cm^2). The counter electrode was Pt gauze, and the reference electrode was a saturated calomel electrode (SCE).

RESULTS AND DISCUSSION

X-ray diffraction of clay films

X-ray diffraction patterns for pillared clay films always exhibited a first order peak in the region $2\theta < 10^0$. This (001) reflection corresponds to the basal spacing of the pillared clays. The values of basal spacing are tabulated in Table 1.

Texas montmorillonite has a basal spacing of 1.24 nm, which corresponds to that of a clay with a monolayer of intercalated water. On heating above 300°C this interlayer of water desorbs and the clay collapses to the thickness of an aluminosilicate layer (0.98 nm) [3a]. To confirm interlamellar penetration of pillaring agent, the basal spacing should exceed that of the aluminosilicate layer. The aluminum-pillared clays after firing in air to at least 300°C have a basal spacing of 1.62–1.80 nm (Table 1). This compares favorably with the values reported in the literature (ca. 1.75 nm) [9]. If one attempts to prepare an aluminum-pillared clay by intercalating only 0.2% of the cation exchange capacity, a gelatinous material is formed with good

TABLE 1

X-ray diffraction data

Clay	Basal spacing [a]/nm	FWHM [b]/°
(1) STx-1	1.24	0.5
(2) STx-1 (heated to 400°C, 3 h)	0.98	–
(3) Al-pillared STx-1 [c]	1.80	0.7
(4) Al-pillared SHCa-1 [c]	1.62	2.0
(5) Si-pillared STx-1 [c]	1.46	1.3
(6) Si-pillared SHCa-1 [c]	1.55	1.0

[a] The distance in nm between repeating 2:1 units of the phyllosilicate structure.

[b] FWHM = full width at one-half maximum peak height expressed in degrees.

[c] All pillared clays were prepared by soaking in pillaring agent for 3–10 h, then heating for 3 h at 300–400°C.

cohesive properties (basal spacing, 1.24–1.36 nm). On heating to 300°C, however, this clay collapses, indicating no extensive interlamellar penetration. The results suggest that small amounts of pillaring agent, although ineffective in maintaining a large basal spacing, might be effective in promoting agglutination; apparently the pillaring agent promotes interparticle binding.

The silicon-pillared clays have a basal spacing in the range, 1.46–1.55 nm (Table 1). This basal spacing is larger than that reported in the literature for clay with a monolayer of siloxane (1.26 nm) [10]. By intercalating $Si(OCH_2CH_3)_4$ directly into the clay, we were able to double the interlamellar spacing. Soaking SHCa-1 for 68 h in $Si(OCH_2CH_3)_4$ yielded an even larger basal spacing (1.67 nm), thus implying that soaking time has a marked effect on interlamellar penetration.

Soaking a silicon-pillared STx-1 in a 1 m*M* $Ru(bpy)_3^{2+}$ solution yielded an orange-colored film. The orange color is characteristic of $[Ru(bpy)_3^{2+}]$ complexes [11]. The basal spacing of the soaked films, 1.52 nm, was essentially the same as that of an unsoaked silicon-pillared clay. Since the diameter of the complex (ca. 0.8 nm) [12]) is too large for effective penetration through the interlamellar aperture (ca. 0.5 nm), the $Ru(bpy)_3^{2+}$ must be incorporated by adsorption on the outside of the clay particles. Quayle and Lunsford [13] noted a similar external adsorption of $Ru(bpy)_3^{2+}$ in Zeolite Y which has a zeolite-lattice-free aperture of 0.74 nm [14]. Hectorite, when fully intercalated with Cu(II) or Fe(II) 1,10-phenanthroline complexes, exhibits an X-ray basal spacing of 1.75 or 1.74 nm, respectively [15]. Space filling models of the complexes show that the cations are approximately 0.8 nm thick (along the C_3 symmetry axis). When the C_3 axis is perpendicular to the silicate sheets, a 1.75 nm spacing should result, and this is in agreement with the data [15a]. Since $Ru(bpy)_3^{2+}$ aligns itself in the same manner as the metal 1,10-phenanthroline complexes [15b], and is about the same thickness (ca. 0.8 nm along the C_3 symmetry axis), the X-ray basal spacing for $Ru(bpy)_3^{2+}$-incorporated hectorite should be about 1.8 nm. This compares favorably with that reported in the literature (1.76 nm) [15c] and determined by us experimentally (1.73 nm). The $Ru(bpy)_3^{2+}$ complex is too large to be intercalated in pillared STx-1 and therefore must be externally adsorbed on the pillared STX-1 particles.

Absorbance spectrophotometry

To evaluate the extent of incorporation of electroactive complex within the clay film, the concentrations of $Ru(bpy)_3^{2+}$ and $Os(bpy)_3^{2+}$ in SHCa-1, and $Os(bpy)_3^{2+}$ in aluminum-pillared SHCa-1 (Al-Hec) and silicon-pillared SHCa-1 (Si-Hec) were determined. Given a molar absorptivity of 21,600 M^{-1} cm^{-1} for $Ru(bpy)_3^{2+}$ in clay [16], the concentration of complex in a saturated, 100 nm hectorite film is about 0.5 *M*. This represents ca. 100% of the cation exchange capacity (c.e.c.) (0.44 mmol univalent cation/g) [17,18], assuming a density of 2 g cm^{-3}. The value is larger than that previously reported for $Ru(bpy)_3^{2+}$ in clay-polyvinyl alcohol (43% of c.e.c.) [4c]. $Os(bpy)_3^{2+}$ in SHCa-1 had a concentration of 0.3 *M* (assuming a molar absorptivity of 1.6×10^4 M^{-1} cm^{-1}), while $Os(bpy)_3^{2+}$ in Al-Hec and Si-Hec had concentrations

of 0.07 *M* and 0.11 *M*, respectively. Thus, pillaring reduces the ability of SHCa-1 to incorporate $Os(bpy)_3^{2+}$, presumably because of the exclusion of the complex from the interlamellar region.

Electrochemistry of clay-modified electrodes

To assess properly the electrochemical properties of clay-modified electrodes, a number of experimental parameters must be optimized or maintained constant; these include: (1) the nature of the clay, (2) the method of purification of the clay and any special pretreatments [4c], (3) the thickness of the film [4c], (4) the concentration of electroactive species within the film, and (5) the nature and concentration of the supporting electrolyte [4c,19]. The distribution of charge within the crystal lattice depends upon the nature of the clay, e.g., a montmorillonite vs. a hectorite [19]. This in turn affects the cation exchange capacity (SHCa-1, c.e.c. = 43.9 mmol univalent cation/100 g; STx-1, c.e.c. = 84.4 mmol univalent cation/100 g) [17]. Even within the montmorillonite class, Wyoming-montmorillonite differs from Texas-montmorillonite in the amount of iron(III) found as an impurity substituted within the octahedral sheet. SWy-1 contains 3.35% (as Fe_2O_3), whereas STx-1 has only 0.65% Fe_2O_3. Hectorite (SHCa-1) has very little iron (0.02% Fe_2O_3) [17]. The amount of iron can affect the ability of the clay to oxidize substrates, e.g., as measured by the intensity of the blue color formed in the benzidine hydrochloride test [3e].

Pretreatment of clay with polyvinyl alcohol tends to increase the apparent diffusion coefficient of intercalated metal bipyridyl complexes. $Ru(bpy)_3^{2+}$ in polyvinylalcohol-impregnated SWy-1 has a D_0 of 10^{-11} cm^2/s [4a] which is much larger than that of metal-bipyridyl complexes in neat STx-1 ($D_0 \sim 1 \times 10^{-12}$ cm^2/s) [4c]. Thus, the clay suspension must be prepared in the same way each time. The thickness of the clay film and the concentration of electroactive species within the film can be maintained constant by spin-coating the clay suspension and then insuring that the film is saturated with electroactive cation.

Finally, the concentration of the supporting electrolyte can also affect the electrochemical activity [4e]. After incorporation of $Fe(bpy)_3^{2+}$ into a thin STx-1 film (100 nm) for 5 min, electrochemical activity was observed in all of the following supporting electrolytes (0.1 *M* LiCl, 0.1 *M* NaCl., 0.1 *M* KCl, 0.1 *M* TMACl, 0.1 *M* TEACl). If more concentrated electrolytes were employed (1 *M* LiCl, 1 *M* NaCl or 1 *M* KCl), the electrochemical activity diminished substantially within 5 min. Apparently, 1 *M* electrolyte solutions ion-exchange with most of the incorporated $Fe(bpy)_3^{2+}$. As long as the concentration of supporting electrolyte was maintained within the range (0.01–0.1 *M*), the electrochemical response for $M(bpy)_3^{2+}$ where $M = Fe^{2+}$, Os^{2+}, Ru^{2+} was unaffected by extended soaking. Figure 2a depicts the CV of $Os(bpy)_3^{2+}$ in SHCa-1 immersed in 0.01 *M* Na_2SO_4. $Ru(NH_3)_6^{3+}$ in SHCa-1, on the other hand, was leached out at a supporting electrolyte concentration of 0.1 *M*, although in 0.01 *M* Na_2SO_4 it produced a wave with a shape much like that of an immobilized or adsorbed monolayer [20] (Fig. 2b). From the expression for peak current for a reversible wave in linear potential sweep voltammetry [20] and plots of

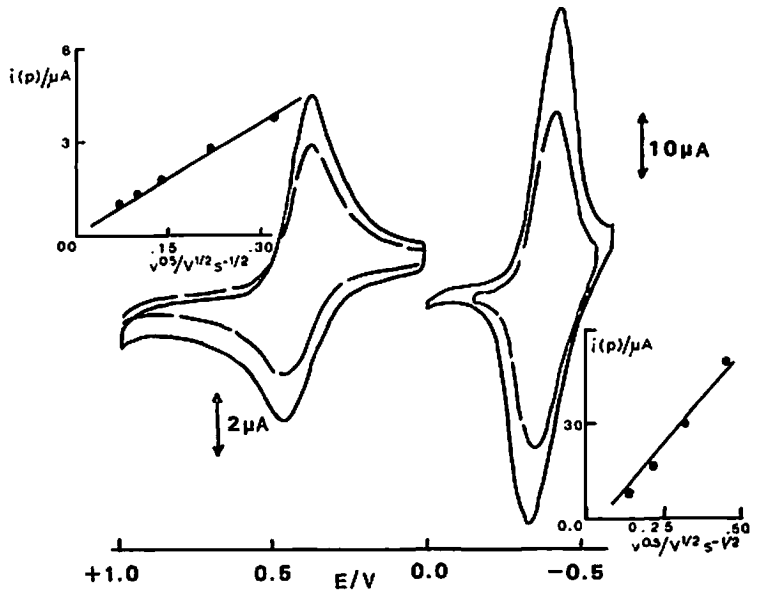

Fig. 2. Cyclic voltammograms at (a) clay(SHCa-1)/$Os(bpy)_3^{2+}$/In_2O_3 and (b) clay (SHCa-1)/$Ru(NH_3)_6^{3+}$/In_2O_3 electrodes in 0.01 *M* Na_2SO_4 as a function of sweep rate; 50 mV s^{-1} (– – –) 100 mV s^{-1} (———). Insets, i_p vs. $v^{1/2}$.

i_p vs. $v^{1/2}$, linear plots were obtained (Fig. 2, inserts), and the apparent diffusion coefficients for $Os(bpy)_3^{2+}$ and $Ru(NH_3)_6^{3+}$ in SHCa-1 were determined (1×10^{-12} cm^2/s and 3×10^{-10} cm^2/s, respectively). D_0 values could also be determined chronocoulometrically from the c_0^* obtained from a CV scan at slow sweep rate, and the slope of the integrated form of the Cottrell equation [20a] (a plot of Q (in μC) vs. $t^{1/2}$). The values obtained for $Os(bpy)_3^{2+}$ and $Ru(NH_3)_6^{3+}$ in SHCa-1 were 2.2×10^{-12} and 3.2×10^{-10} cm^2 s^{-1}, respectively.

Table 2 lists CV data on the surface coverage, Γ, and concentration within the film, c_0, for a number of metal complexes in SHCa-1 or STx-1. The values of D_0 obtained using CV and chronocoulometry are also tabulated. Some general features of these results are: (1) for saturated films, the surface coverage varies between 3 and 11×10^{-10} mol cm^{-2}, and the film concentration is 0.07 to 0.12 mol dm^{-3} of electroactive species, irrespective of clay or metal complex. (2) The apparent diffusion coefficients of $Ru(bpy)_3^{2+}$ and $Os(bpy)_3^{2+}$ in both SHCa-1 and STx-1 are ca. 1 to 2×10^{-12} cm^2 s^{-1}, while those of $Co(bpy)_3^{2+}$ and $Fe(bpy)_3^{2+}$ are lower, suggesting that electron exchange, which is slower with these species than with the Ru and Os complexes, may play a role in charge transport in clay [21].

The value for $Os(bpy)_3^{2+}$ in SHCa-1 contrasts with the value (3.5×10^{-11} cm^2 s^{-1}) obtained for $Os(bpy)_3^{2+}$ in SWy-1 [5a]. Since the nature of the supporting electrolyte may affect D_0, the differences in the diffusion coefficient when using sulfate as compared to acetate may be due to ion pairing between $M(bpy)_3^{2+}$ and

TABLE 2

Electrochemistry at clay-modified electrodes ($d = 10^2$ nm)

Clay	Metal complex	$10^{10}\ \Gamma$/ mol cm^{-2} [a]	c_0/ mol dm^{-3} [a]	$10^{12}\ D_0$/ cm^2 s^{-1} [b]	$10^{12}\ D_0$/ cm^2 s^{-1} [c]
SHCa-1	$Ru(bpy)_3^{2+}$	6.7	0.07	–	1.0
SHCa-1	$Os(bpy)_3^{2+}$	11	0.1	1	2.2
SHCa-1	$Co(bpy)_3^{2+}$	1.9 [d]	0.044 [d]	1 [d]	0.16
STx-1	$Os(bpy)_3^{2+}$	3.0	0.1 [e]	1 [e][4c]	1.0
STx-1	$Fe(bpy)_3^{2+}$	7.3	0.12 [e]	1 [e]	0.41
SHCa-1	$Ru(NH_3)_6^{3+}$ [f]	11	0.11	290	320 [g]
SHCa-1	$Ru(NH_3)_6^{3+}$ [h]	11	0.11	300	–

[a] Value determined from cyclic voltammetry with $v = 5$ mV/s.
[b] D_0 obtained from CV.
[c] D_0 obtained using chronocoulometry, c_0 assumed to be 0.1 M unless otherwise specified.
[d] Film was not saturated with $Co(bpy)_3^{2+}$.
[e] Film thickness was 50 nm.
[f] Concentration of soaking solution (1×10^{-3} M).
[g] $c_0 = 0.73$ M.
[h] Concentration of soaking solution (5×10^{-3} M).

SO_4^{2-} ion, within the montmorillonite [15c]. (3) The diffusion coefficient of $Ru(NH_3)_6^{3+}$ (ca. 3×10^{-10} cm^2/s) is 2 orders of magnitude larger than that of the bpy species. $Ru(NH_3)_6^{3+}$ is much smaller than $Ru(bpy)_3^{2+}$ and therefore would be expected to diffuse more rapidly within the clay because of its ready access to narrow channels. The facile penetration of $Ru(NH_3)_6^{3+}$ into zeolite Y has already been reported [13]. (4) The concentration of $Ru(NH_3)_6^{3+}$ in SHCa-1 is independent of the concentration of soaking solution (within the range 1 to 5×10^{-3} M), indicating that saturation of the clay has been achieved.

The film concentration (ca. 0.1 M) determined by CV represents only 15–30% of the total concentration as determined by absorbance spectrophotometry. This value corresponds well with that previously reported (ca. 18%) [4c], and indicates that most of the incorporated metal complex is not involved in charge transfer. The external surface area of SHCa-1 (as measured by N_2 BET) is 63.2 m^{2}g^{-1}, which represents 13% of the total surface area (486 m^2 g^{-1}) [17]. Similarly, STx-1 has a N_2 BET surface area of 83.8 m^2 g^{-1}, representing 14% of the total (599 m^2 g^{-1}) [17]. The N_2 BET surface determination only measures the area outside the interlamellar region, since the preliminary outgassing procedure removes intercalated water and causes the clay to collapse [17]. The fact that the fraction of electroactive complex (15–30%) is similar to the fractional surface area (13–14%) suggests that an externally adsorbed complex is the primary contributor to charge transport in clay-modified electrodes (as it must be in pillared-clay modified electrodes).

Further evidence indicating that an intercalated complex is electrochemically silent stems from a series of experiments with mixtures of incorporated complexes (a mixed electrode) [22]. If SHCa-1 is soaked in 1 mM $Ru(bpy)_3^{2+}$ for 1 h, then

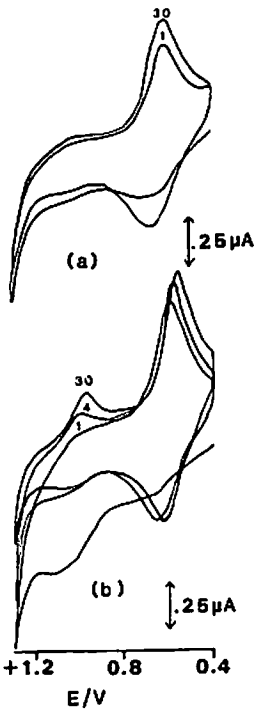

Fig. 3. Cyclic voltammograms at (a) clay (SHCa-1)/$Ru(bpy)_3^{2+}$, $Os(bpy)_3^{2+}/In_2O_3$ electrode (fresh) and (b) clay (SHCa-1)/$Ru(bpy)_3^{2+}$, $Os(bpy)_3^{2+}/In_2O_3$ electrode (air-dried, 4 h). The numbers refer to scan after immersion into 0.026 *M* $(NaPO_3)_6$ + 0.06 *M* Na_2SO_4, scan rate = 50 mV s^{-1}.

immersed in 0.1 *M* Na_2SO_4, the CV displays the typical wave form reported previously [4c]. On the first scan, the anodic peak current, i_{pa}, is large and then subsequently decreases on repetitive cycling, reaching a steady state after about 10 scans [4c]. The ratio of cathodic peak current to anodic peak current (i_{pc}/i_{pa}) approaches 1 both on continuous scanning, and as the scan rate (v) increases. If the $Ru(bpy)_3^{2+}$ soaked electrode is then immersed in 1 m*M* $Os(bpy)_3^{2+}$ for 3 days, rinsed, immersed in supporting electrolyte, then cycled 30 times until a steady state CV is obtained, the $Ru(bpy)_3^{2+}$ wave at $E^\circ = 1.0$ V vs. SCE has virtually disappeared, while the $Os(bpy)_3^{2+}$ wave at $E^\circ = 0.65$ V vs. SCE now dominates (Fig. 3a). If the mixed electrode is removed and air-dried for 4 h and then cycled in supporting electrolyte, there is a marked change in the appearance of the voltammogram. The i_{pc} for $Ru(bpy)_3^{2+}$ (and to a smaller extent that for $Os(bpy)_3^{2+}$) has increased substantially, approaching a steady state after 35 scans (Fig. 3b). Concomitantly, there is a roughening of the surface texture. Apparently, the $Ru(bpy)_3^{2+}$, which was the first species to be intercalated within the SHCa-1, is embedded within the interlamellar region, with the more accessible $Ru(bpy)_3^{2+}$ exchanged during the $Os(bpy)_3^{2+}$ soak. After air-drying, the clay is susceptible to cracking, and begins to

roughen on continuous cycling, thus exposing the more deeply imbedded $Ru(bpy)_3^{2+}$. More $Ru(bpy)_3^{2+}$ (and $Os(bpy)_3^{2+}$) complexes are now close to edges and can therefore exhibit electrochemical activity. Although the mixed electrode results are not conclusive, they do support the hypothesis that the externally adsorbed complex is electroactive and that the deeply intercalated complex $M(bpy)_3^{2+}$ is not involved in charge transport through the clay film.

Electrochemistry of pillard-clay modified electrodes

Two different pillaring agents were used to fix the basal spacing of either STx-1 or SHCa-1. The aluminum pillaring agent is a hydrated hydroxy cation, $Al_{13}O_4(OH)_{28+n}^{(3-n)}$, which neutralizes some of the positive charge deficiency in the layers of the smectite. Presumably the cations are uniformly distributed on the interlayer surfaces [2], but are not chemically bound to the silicate sheets [9b]. The silicon pillaring agent, $Si(OC_2H_5)_4$, is a neutral hydrolyzable silane, that can permeate into the interlamellar region, where it is apparently hydrolyzed in situ by adsorbed water.

Figures 4 and 5 depict the cyclic voltammograms, obtained at different scan rates, for $Os(bpy)_3^{2+}$ incorporated into Al-Hec and Si-Hec thin clay films in 0.01 *M* Na_2SO_4, respectively. Note the large differance in i_{pc} (cathodic peak current) at a given scan rate for the two different systems. The i_{pc} for $Os(pby)_3^{2+}$ in Si-Hec is about 4 times that for $Os(bpy)_3^{2+}$ in Al-Hec. Similar results were also observed for $Fe(bpy)_3^{2+}$ in Si-STx-1 when compared with $Fe(bpy)_3^{2+}$ in Al-STx-1. In each case, the i_{pc} for the silicon-pillared clay is higher than that for the aluminum-pillared clay. Plots of i_p vs. $v^{1/2}$ (Figs. 4 and 5, insets), yielded D_0's for $Os(bpy)_3^{2+}$ in Si-Hec and Al-Hec of 3×10^{-12} and 5×10^{-12} cm^2 s^{-1}, respectively. The value for $Os(bpy)_3^{2+}$ in Si-Hec, as determined from chronocoulometry, was slightly higher (1.3×10^{-11} cm^2 s^{-1}). Table 3 contains the surface coverages, Γ, film concentrations, c_0 and diffusion coefficients, D_0 (from CV and chronocoulometry) for a number of electroactive cations incorporated into pillared clays. Some features are readily apparent: (1) the film concentration of electroactive cation (as determined by integration of the cathodic current at $v = 5$ mV/s for $M(bpy)_3^{2+}$ and 20 mV/s for $Ru(NH_3)_6^{3+}$ is much lower for pillared clays, ranging from 0.001 to 0.061 *M* for Al-Hec and 0.013 to 0.065 *M* for Si-Hec, than it is for unpillared clays (0.07 to 0.12 *M*). Both pillaring agents apparently block the interlamellar region, making it less accessible to $M(bpy)_3^{2+}$ complexes. (2) The Al-Hec generally incorporates less electroactive cation than Si-Hec. Since the aluminum pillaring agent neutralizes some of the cation exchange sites, this should then reduce the amount of externally adsorbed complex. (3) The D_0 for $Ru(NH_3)_6^{3+}$ in Al-Hec or Si-Hec is about the same as that for $Ru(NH_3)_6^{3+}$ in SHCa-1. Apparently pillaring does not affect the mobility of $Ru(NH_3)_6^{3+}$ within the clay to any great extent. When the clay is substantially pillared (as shown by a low value for c_0) the D_0 for $Ru(NH_3)_6^{3+}$ may be lower.

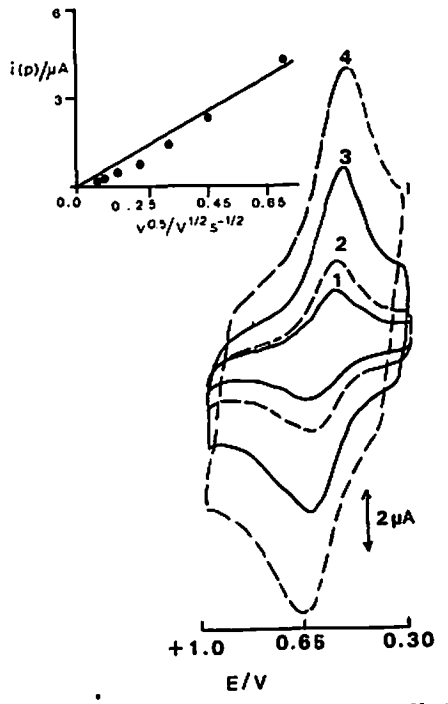

Fig. 4. Cyclic voltammogram at clay (Al-Hec)/$Os(bpy)_3^{2+}$/In_2O_3 electrode in 0.01 *M* Na_2SO_4 as a function of sweep rate. Scan rate: (1) 100, (2) 200, (3) 500, (4) 1000 mV s^{-1}. Inset, i_p vs. $v^{1/2}$.

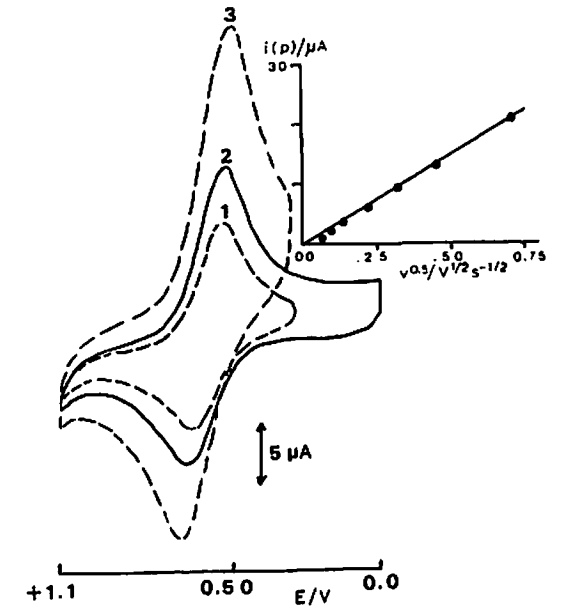

Fig. 5. Cyclic voltammogram at clay (Si-Hec)/$Os(bpy)_3^{2+}$/In_2O_3 electrode in 0.01 *M* Na_2SO_4 as a function of sweep rate. Scan rate: (1) 100 (2) 200, (3) 500 mV s^{-1}. Inset, i_p vs. $v^{1/2}$.

TABLE 3

Electrochemistry of pillared-clay modified electrodes (d = 10^2 nm)

Clay	Metal complex	$10^{10}\ \Gamma$ [a]/ mol cm^{-2}	c_0 [a]/ mol dm^{-3}	$10^{12}\ D_0$ [a] cm^2 s^{-1}	$10^{12}\ D_0$ [b]/ cm^2 s^{-1}
Fe-STx-1	$Fe(bpy)_3^{2+}$	2.3	0.023 [c]	1	-
Al-STx-1	$Fe(bpy)_3^{2+}$	[f]	0.01 [c]	-	-
Al-STx-1	$Fe(bpy)_3^{2+}$	0.1 [d]	0.002 [d,e]	-	-
Al-Hec	$Fe(bpy)_3^{2+}$	0.086	0.001	-	-
Al-Hec	$Os(bpy)_3^{2+}$	1.4	0.014	5	-
Al-Hec	$Ru(NH_3)_6^{3+}$	6.1	0.061	-	710
Al-Hec	$Ru(NH_3)_6^{3+}$	1.8	0.018	80	-
Si-STx-1	$Fe(bpy)_3^{2+}$	2.9	0.05	9	-
Si-SWy-1	$Os(bpy)_3^{2+}$	1.3	0.013	-	-
Si-Hec	$Os(bpy)_3^{2+}$	4.0	0.040	-	13
Si-Hec	$Os(bpy)_3^{2+}$	6.5	0.065	3	-
Si-Hec	$Ru(NH_3)_6^{3+}$	4.3	0.043	-	550

[a] Value determined from cyclic voltammetry.
[b] D_0 obtained using chronocoulometry, c_0 determined from CV.
[c] Calculated from information in reference 4e.
[d] Clay was soaked for 16 h in $[Al(OH)_2Cl]_x$.
[e] Film thickness was 50 nm.

Finally, the soaking time of the clay in pillaring agent has a profound effect on the subsequent incorporation of electroactive cation. If STx-1 is soaked for 16 h in aluminum pillaring agent, little if any $M(bpy)_3^{2+}$ can subsequently be incorporated. Concurrently, with extended soaking the penetration of $Fe(CN)_6^{4-}$ in 0.1 *M* Na_2SO_4 at a thin Al-STx-1 electrode was ca. 30% of that observed at the corresponding unpillared STx-1 electrode. The same sort of attenuation was also observed for a Si-STx-1 electrode immersed in 5 m*M* $Fe(CN)_6^{4-}$ in 0.1 *M* Na_2SO_4. Apparently, pillaring affects not only the incorporation of cationic complexes, but also the permeability of anions within the interparticle region [4e].

Redox activity of smectite clays

A previous report from this laboratory suggested that $Ru(bpy)_3^{3+}$, a strong electron acceptor (E° = 1.0 V vs. SCE), can abstract electrons from initially reduced SWy-1, acting as an electron donor [4c]. Reduction of the uncharged TCNE molecule by ferrous ions within the lattice framework of montmorillonite has been reported to give rise to the red TCNE radical anion intermediate [3a,d]. Oxidation of benzidine hydrochloride by ferric ion in montmorillonite has also been observed [3a,e,23]. The literature thus indicates a possible charge transfer role for iron species in montmorillonite clays.

During CV, $Ru(bpy)_3^{2+}$, and to a smaller extent, $Fe(bpy)_3^{2+}$, exhibit enhanced anodic peak currents with a smaller cathodic peak on scan reversal after incorpora-

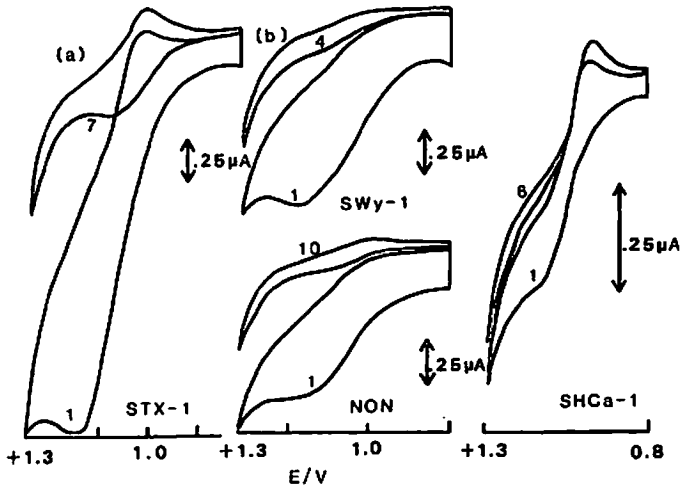

Fig. 6. Cyclic voltammograms at (a) clay(STx-1)/Ru(bpy)$_3^{2+}$/In_2O_3; (b) clay (SWy-1)/Ru(bpy)$_3^{2+}$/In_2O_3; (c) clay (nontronite)/Ru(bpy)$_3^{2+}$/In_2O_3 electrodes and (d) clay(SHCa-1)/Ru(bpy)$_3^{2+}$/In_2O_3 in 0.1 *M* Na_2SO_4; sweep rate: 10 mV s^{-1}. Film thickness ca. 100 nm for (a-c), 1 μm for (d), films soaked for ca. 1 h in 1 m*M* Ru(bpy)$_3^{2+}$.

tion into SWy-1 [4c]. SWy-1 has a high iron content (3.35% Fe_2O_3, 0.32% FeO) [17] and so Fe(II) in the lattice might regenerate Ru(bpy)$_3^{2+}$ or Fe(bpy)$_3^{2+}$ [24] after their electrochemical oxidation to Ru(bpy)$_3^{3+}$ and Fe(bpy)$_3^{3+}$, respectively (a catalytic or EC′-type mechanism) [20a,24]. To determine whether iron(II) could be the cause of the enhanced anodic wave, Ru(bpy)$_3^{2+}$ was incorporated into four different clays (STx-1, SWy-1, the low iron SHCa-1, and nontronite, a clay with iron extensively incorporated into the tetrahedral sites of a 2:1 phyllosilicate). Figure 6 depicts the cyclic voltammograms for the Ru(bpy)$_3^{2+}$ incorporated clays immersed in 0.1 *M* Na_2SO_4. The results can be summarized as follows: (1) the i_{pa} is difficult to determine because of the background current. To a first approximation, i_{pa} seems to be largest for STx-1 and SWy-1 (Figs. 6a and b, respectively). Both of these clays had been freeze-dried. (2) STx-1 and SHCa-1 (Figs. 6a and d, respectively) both exhibit a cathodic wave on the first and subsequent scans. These two clays have the smallest amounts of iron. (3) The i_{pc}/i_{pa} ratio appears to approach zero for SWy-1 and nontronite (Figs. 6b and c), both of which contain an appreciable amount of iron impurity. In fact, there appears to be an inverse relation between i_{pc}/i_{pa} and iron content, i.e., as the percent of iron impurity increases, i_{pc}/i_{pa} approaches zero. Naturally any special oxidizing (heating in air) or reducing (reacting with $SnCl_2$) pretreatments of the clay can markedly affect the i_{pc}/i_{pa} ratio. Thus, we propose the reaction mechanism:

$$Ru(bpy)_3^{2+} \rightarrow Ru(bpy)_3^{3+} + e^-$$

$$Ru(bpy)_3^{3+} + Fe(II)_{lattice} \rightarrow Ru(bpy)_3^{2+} + Fe(III)_{lattice}$$

An additional piece of experimental evidence which suggests a role for iron in the redox chemistry of metal-complex-impregnated-clays stems from a series of mediation experiments employing $Ru(bpy)_3^{2+}$ and $Ru(NH_3)_6^{3+}$. One common feature shared by intercalated $Ru(bpy)_3^{2+}$ and octahedral Fe within a clay film is that both are relatively immobile. $Ru(bpy)_3^{2+}$ diffuses slowly ($D_0 \sim 10^{-12}$ cm^2 s^{-1}) while the lattice iron is immobile and not readily removed even by pretreatment with citrate and dithionite [25]. A CV for $Ru(bpy)_3^{2+}$ can be observed directly because it is adsorbed on the external surfaces and does diffuse, whereas the redox behavior of octahedral iron can only be inferred by its effects on the redox potential or current density of other incorporated electroactive species (such as $Ru(bpy)_3^{2+}$). To enhance the electroactivity of immobile iron and observe the redox behavior directly, electron transfer to and from the octahedral iron must be facilitated. One approach that has been effective is to use a rapidly diffusing redox reagent (mediator) such as $Ru(NH_3)_6^{3+}$, which can shuttle electrons between the electrode surface and the immobilized metal or metal complex [26].

In a series of experiments with either STx-1 or SHCa-1 modified electrodes, we first incorporated $Ru(NH_3)_6^{3+}$ and observed its electroactivity. The CV for $Ru(NH_3)_6^{3+}$ in SHCa-1 was similar to that in Fig. 2b. $Ru(bpy)_3^{2+}$ was then incorporated to see if any mediation between $Ru(NH_3)_6^{3+}$ and $Ru(bpy)_3^{2+}$ could be observed. The results indicated that $Ru(bpy)_3^{2+}$ replaced much of the $Ru(NH_3)_6^{3+}$

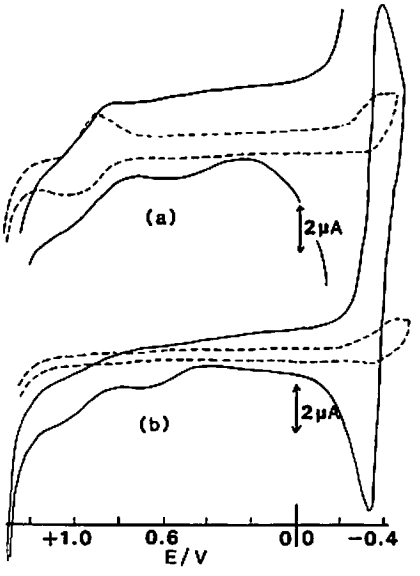

Fig. 7. Cyclic voltammograms at (a) clay (SHCa-1)/$Ru(NH_3)_6^{3+}$, $Ru(bpy)_3^{2+}/In_2O_3$ electrode in (– – –) 0.01 *M* Na_2SO_4, in (———) ca. 10^{-5} *M* $Ru(NH_3)_6^{3+}$:0.01 *M* Na_2SO_4 and (b) clay (STx-1)/$Ru(NH_3)_6^{3+}$, $Ru(bpy)_3^{2+}/In_2O_3$ electrode in (– – –) 0.01 *M* Na_2SO_4, in (———) 5×10^{-4} *M* $Ru(NH_3)_6^{3+}$ +0.01 *M* Na_2SO_4.

(Fig. 7a, dashed line). If the mixed electrode (containing both $Ru(NH_3)_6^{3+}$ and $Ru(bpy)_3^{2+}$) was then immersed in a solution of $Ru(NH_3)_6^{3+}$ in 0.01 *M* Na_2SO_4, the i_{pc} due to $Ru(NH_3)_6^{3+}$ increased dramatically, as expected. On repetitive scanning two anodic waves at +1.0 V and +0.6 V vs. SCE increased in size. Simultaneously, the cathodic wave for $Ru(NH_3)_6^{3+}$ (ca. −0.4 V) also increased in size (Fig. 7b). The results indicate that $Ru(NH_3)_6^{3+}$ is functioning as an efficient mediator enhancing the rate of electron transfer to and from $Ru(bpy)_3^{2+}$ and an unknown substituent with a redox potential of ca. 0.6 V vs. SCE. Smectite clays have two potential oxidizing sites (planer ferric ion and edge alumina) [3d,e]; however, the clay has only one reductant (planar ferrous ion). Since a reductant is implicated in the enhancement of the anodic wave for $Ru(bpy)_3^{2+}$, and since octahedral iron might be expected to have a redox potential of about +0.6 V vs. SCE [20a], we attribute the new wave to planar iron, and propose the reaction mechanism:

$$Ru(NH_3)_6^{3+} + e^- \rightarrow Ru(NH_3)_6^{2+}$$

$$Ru(NH_3)_6^{2+} + Fe(III)_{lattice} \rightarrow Ru(NH_3)_6^{3+} + Fe(II)_{lattice}$$

CONCLUSIONS

Some of the most important observations stemming from the present work are:

(1) Pillaring with oxycations of aluminum and silicon reduces the capacity for incorporation of electroactive ions of smectite clays. Alumina reduces the c.e.c. by charge neutralization, whereas silica pillaring reduces the accessibility of the interlamellar region.

(2) Metal bipyridyl complexes can be adsorbed but not intercalated within silicon-pillared clays, because of steric constraints. However, the impregnated smectites show good electrochemical response. The results indicate that externally adsorbed bipyridyl complexes maintain charge transport within the clay film.

(3) The basal spacing seems to have little effect on the mobility of metal bipyridyl complexes.

(4) $Ru(NH_3)_6^{3+}$ readily diffuses through pillared and unpillared clays and has a diffusion coefficient of the order of 10^{-10} cm^2 s^{-1}. Apparently the small size of the metal chelate allows it to penetrate readily into the interlamellar region.

(5) About 15–30% of the impregnated metal complexes are electroactive, suggesting that the majority can not diffuse to the electrode surface.

(6) Octahedral iron within the alumino-silicate layer is involved in charge transfer reactions and may exchange electrons with electroactive cations.

Based on the results, a tentative model can be proposed for charge transport within pillared clay-modified electrodes. For large metal complexes, charge transport is primarily due to the diffusion of externally adsorbed species. For $Ru(NH_3)_6^{3+}$ charge transport is due to the physical diffusion both through and around the

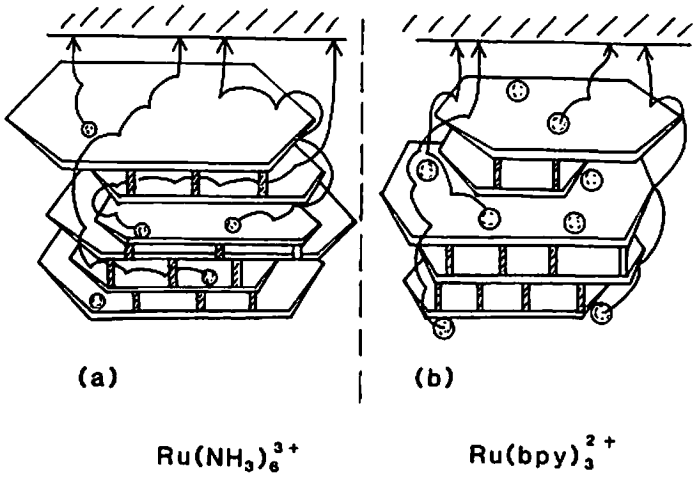

Fig. 8. Diagram illustrating the possible locations and diffusive pathways of (a) $Ru(NH_3)_6^{3+}$ and (b) $Ru(bpy)_3^{2+}$ impregnated smectites on an electrode surface. The layered clays have been represented as hexagonal platelets because of previous scanning electron microscopy studies [17].

aluminosilicate sheets. Figure 8 illustrates a schematic model of transport for $Ru(NH_3)_6^{3+}$ and $Ru(bpy)_3^{2+}$ in Si-Hec.

ACKNOWLEDGEMENTS

The support of the National Science Foundation (CHE 8402135) is gratefully acknowledged. We also appreciate the help of Dr. H. Hartman in supplying the sample of nontronite. W.E.R. would also like to thank Jean-Francois Equey and H.-Y. Liu for many helpful discussions.

REFERENCES

1 H. van Olphen, An Introduction to Clay Colloid Chemistry, 2nd ed., Wiley, New York, 1977.
2 T.J. Pinnavaia, Science, 220 (1983) 365.
3 (a) B.K.G. Theng, The Chemistry of Clay-Organic Reactions, Adam Hilger, London, 1974; (b) B.K.G. Theng, Clays Clay Miner., 19 (1971) 383; (c) H. Van Damme, F. Obrecht and M. Letellier, Nouv. J. Chim., 8 (1984) 681; (d) D.H. Solomon, B.C. Loft and J.D. Swift, Clay Miner., 7, (1968) 399; (e) D.H. Solomon, B.C. Loft and J.D. Swift, Clay Miner., 7 (1968) 389.
4 (a) P.K. Ghosh and A.J. Bard, J. Am. Chem. Soc., 105 (1983) 5691; (b) P.K. Ghosh, A.W.H. Mau and A.J. Bard, J. Electroanal. Chem., 169 (1984) 315; (c) D. Ege, P.K. Ghosh, J.R. White, J.F. Equey and A.J. Bard, J. Am. Chem. Soc., 107 (1985) 5644; (d) J.R. White and A.J. Bard, J. Electroanal. Chem., 197 (1986) 233; (e) K. Itaya and A.J. Bard, J. Phys. Chem., in press.
5 (a) H.-Y. Liu and F.C. Anson, J. Electroanal. Chem., 184 (1985) 411; (b) A. Yamagishi and A. Aramata, J. Chem. Soc., Chem. Comm., (1984) 452.
6 J.J. Fripiat, A.N. Jelli, G. Poncelot and J. Andre, J. Phys. Chem., 69 (1965) 2185.
7 (a) J.G. Gaudiello, D.G. Bradley, K.A. Norton, W.H. Woodruff and A.J. Bard, Inorg. Chem. 23, (1984) 3; (b) N.H. Furman and C.O. Miller, Inorg. Synth., 3 (1950) 160.

8 G.W. Brindley and R.E. Sempels, Clay Miner., 12 (1977) 229.
9 (a) N. Lahav, U. Shani and J. Shabtai, Clays Clay Miner., 26 (1978) 107; (b) D. Plee, F. Borg, L. Gatineau and J.J. Fripiat, J. Am. Chem. Soc., 107 (1985) 2362.
10 T. Endo, M.M. Mortland and T.J. Pinnavaia, Clays Clay Miner., 28 (1980) 105.
11 R.A. Palmer and T.S. Piper, Inorg. Chem., 5 (1966) 864.
12 D.P. Rillema, D.S. Jones and H.A. Levy, J. Chem. Soc., Chem. Commun., 849 (1979).
13 W.H. Quayle and J.H. Lunsford, Inorg. Chem., 21 (1982) 97.
14 D.W. Breck, Zeolite Molecular Sieves, Wiley, New York, 1974, p. 177.
15 (a) V.E. Berkheiser and M.M. Mortland, Clays Clay Miner., 25 (1977) 105; (b) S. Abdo, P. Canesson, M. Cruz, J.J. Fripiat and H. Van Damme, J. Phys. Chem., 85 (1981) 797; (c) F.S.E. Traynor, M.M. Mortland and T.J. Pinnavaia, Clay Clay Miner., 26 (1978) 318.
16 P.K. Ghosh and A.J. Bard, J. Phys. Chem., 88 (1984) 5519.
17 H. Van Olphen and J.J. Fripiat (Eds.) Data Handbook for Clay Materials and other Non-Metallic Minerals, Pergamon Press, New York, 1979.
18 D. Krenske, S. Abdo, H. Van Damme, M. Cruz and J.J. Fripiat, J. Phys. Chem., 84 (1980) 2447.
19 A. Hahti, D. Keravis, P. Levitz and H. Van Damme, J. Chem. Soc., Faraday Trans. 2, 80 (1984) 67.
20 (a) A.J. Bard and L.R. Faulkner, Electrochemical Methods, Fundamentals and Applications, Wiley, New York, 1980, Ch. 12; (b) R.W. Murray, Chemically Modified Electrodes, in A.J. Bard (Ed.), Electroanalytical Chemistry, Marcel Dekker, New York, 1984, Ch. 13.
21 D.A. Buttry and F.C. Anson, J. Am. Chem. Soc., 105 (1983) 685.
22 H.S. White, J. Leddy and A.J. Bard, J. Am. Chem. Soc., 104 (1982) 4811.
23 D. Kruger and F. Oberlies, Naturwissenschaften, 31 (1943) 92.
24 R.S. Nicholson and I. Shain, Anal. Chem., 36 (1964) 706.
25 O.P. Mehra, M.L. Jackson, Clays Clay Miner., Proc. Conf., 7 (1958) 317.
26 D.A. Buttry and F.C. Anson, J. Am. Chem. Soc., 106 (1984) 59; (b) M. Fukui, A. Kitani, C. Degrand and L.L. Miller, J. Am. Chem. Soc., 104 (1982) 28.